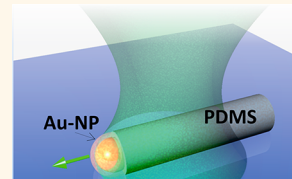


Nanolithography by Plasmonic Heating and Optical Manipulation of Gold Nanoparticles

Michael Fedoruk, Marco Meixner, Sol Carretero-Palacios, Theobald Lohmüller,* and Jochen Feldmann

Photonics and Optoelectronics Group, Department of Physics and CeNS, Ludwig-Maximilians-Universität München, Amalienstraße 54, 80799 Munich, Germany

ABSTRACT Noble-metal particles feature intriguing optical properties, which can be utilized to manipulate them by means of light. Light absorbed by gold nanoparticles, for example, is very efficiently converted into heat, and single particles can thus be used as a fine tool to apply heat to a nanoscopic area. At the same time, gold nanoparticles are subject to optical forces when they are irradiated with a focused laser beam, which renders it possible to print, manipulate, and optically trap them in two and three dimensions. Here, we demonstrate how these properties can be used to control the polymerization reaction and thermal curing of polydimethylsiloxane (PDMS) at the nanoscale and how these findings can be applied to synthesize polymer nanostructures such as particles and nanowires with subdiffraction limited resolution.



KEYWORDS: gold nanoparticles · plasmonic heating · optical forces · polymers

The pursuit to make nanofabrication faster and simpler has inspired numerous innovations for patterning materials on a small scale.¹ Scanning probe lithography based methods are a particularly intriguing example of this development. Individual molecules^{2,3} and even single atoms⁴ can be positioned with the tip of an AFM or STM. Likewise, the tip can be used to remove material by mechanical force,⁵ anodic oxidation,⁶ thermal manipulation,^{5,7} or near-field illumination of the underlying surface.^{8,9} In all of these cases, the pattern is directly “written” into the surface of a sample. Due to their serial nature, these methods usually suffer from being slow, but introducing massively parallel tip arrays on a single cantilever has led to a tremendous increase of sample throughput rates.¹⁰ Today, scanning probe methods represent an almost common route for nanofabrication on a scale below 100 nm and have become competitive with standard top-down nanofabrication technologies such as electron beam¹¹ or focused ion beam lithography.¹² The challenge for all scanning probe methods, however, remains that the interaction between the scanning probe and the substrate is controlled mechanically and the probe, such as a rigid AFM cantilever, is always physically attached to a

scanning head or control unit. In this report, we demonstrate an approach to bypass this functional requirement. We introduce a new concept for optical nanolithography by using a single gold particle for nanofabrication that is controlled and steered all-optically with a focused laser beam.

Noble-metal particles show distinct plasmonic properties that can be utilized to manipulate them by means of light.¹³ Light absorbed by gold nanoparticles is very efficiently converted into heat, and temperatures up to several hundred degrees centigrade can be reached within nanoseconds.¹⁴ Gold particles can thus be used as a fine tool to apply heat to a nanoscopic area. In this context, plasmonic heating has been used for biomedical and analytical applications such as photothermal destruction of tumor cells¹⁵ and high-throughput DNA analysis.¹⁶ Recently, some attention has been given to the possibility to employ controlled heating for nanolithography or nanochemistry purposes.^{17–19} At the same time, gold nanoparticles are also subject to optical forces when they are irradiated with a laser. These forces include the scattering force originating from momentum transfer of scattered or absorbed photons and the gradient force which is proportional to the intensity gradient of the Gaussian beam.²⁰ Both

* Address correspondence to t.lohmueler@lmu.de.

Received for review April 28, 2013 and accepted August 13, 2013.

Published online August 13, 2013
10.1021/nn402124p

© 2013 American Chemical Society

optical forces can be used to print, manipulate, and trap gold and silver particles in two and three dimensions by means of light.^{21–23}

In this paper, we take advantage of the properties arising from the nanoparticle–light interactions mentioned above to demonstrate their application potential for nanofabrication. We report how gold nanoparticles can be used as fine tools to control heat-induced polymerization reactions at the nanoscale. The applicability of this approach as a concept for nanolithography is demonstrated by the controlled synthesis of polydimethylsiloxane (PDMS) polymer nanoparticles and nanowires.

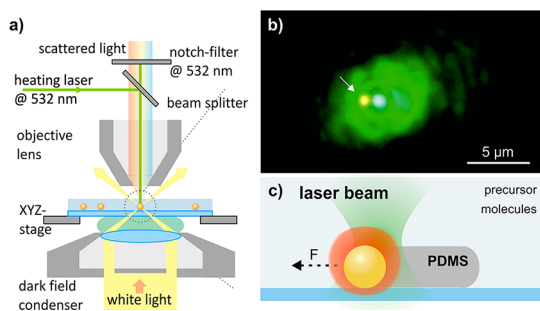


Figure 1. (a) Schematic overview of the experimental setup. (b) Dark field image of a single 82 nm gold nanoparticle next to the focus of a 532 nm laser beam (the extinction spectrum of the gold particles is shown in the Supporting Information, Figure S1). (c) Schematic illustration of the nanofabrication process. The particle is heated and moved at the same time through the fluid polymer precursor. A PDMS polymer shell is formed due to thermal curing along the nanoparticle track.

RESULTS AND DISCUSSION

A schematic illustration of the experimental approach is shown in Figure 1. A clean glass cover slip was decorated with gold nanoparticles by drop-casting a particle solution onto the substrate. After a few minutes the sample was rinsed with water and blow-dried with nitrogen. In the next step, the substrate was spin-coated with a 10:1 mixture of PDMS precursor molecules and the curing agent. PDMS was chosen as a model system, because it is optically transparent and has an outstanding chemical and biological compatibility, making it one of the most widely used polymer materials in science and research.²⁴ Also, the polymerization reaction of PDMS is controlled by heat. Thermal curing of PDMS takes about 1 day at room temperature but can be significantly accelerated with increasing temperatures.²⁵

Dark field microscopy was used to detect and localize the individual gold particles on the glass substrate by their scattered light. Then, a 532 nm laser beam was coupled into the microscope and focused onto the gold nanoparticles on the sample in order to heat the particles and to start the thermal curing reaction (Figure 1b,c).

At first we studied the heat-induced polymerization of PDMS as a function of the exposure time and the laser power (Figure 2). A series of experiments were performed by irradiating several particles of the same size at a constant laser power of 2 mW and an increasing exposure time between 1 and 16 s. After the laser exposure, the sample was rinsed with hexane to

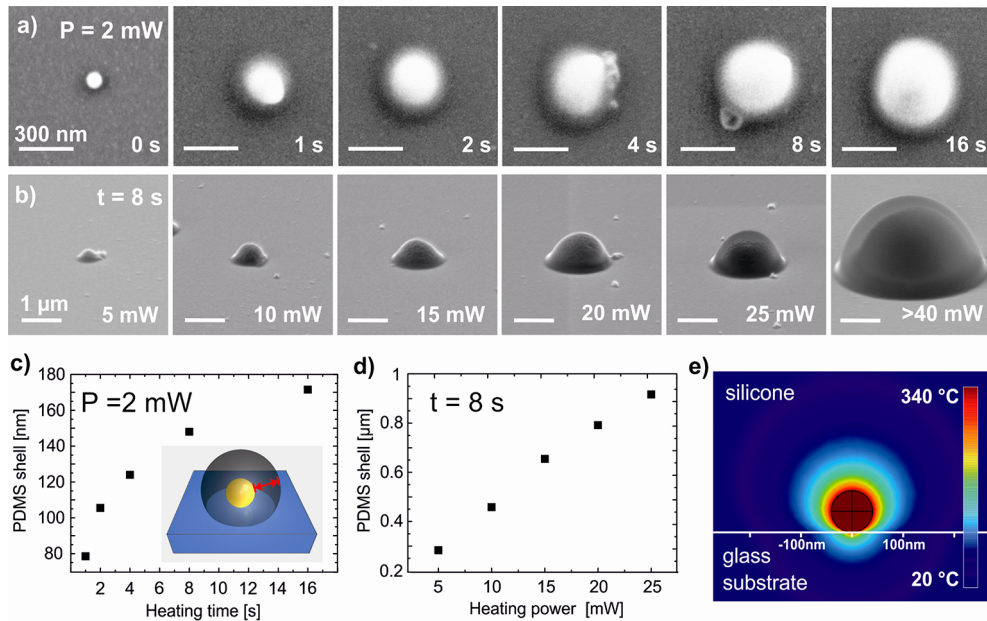


Figure 2. Effect of the laser-mediated particle heating on the thermal curing of PDMS. (a) SEM micrographs of the PDMS structures formed with a 2 mW laser for an increasing exposure time between 1 and 16 s. (b) Side view SEM micrographs of the PDMS structures for a constant exposure time of 8 s and an increasing laser power between 2.5 and 12.5 mW and around 20 mW (micrographs are taken with a 60° angle). (c) Dependence of the PDMS shell thickness on the heating time for a constant laser power of 2 mW. (d) Increasing PDMS shell thickness vs laser power for 8 s exposure. (e) Simulation of the heat distribution of an 82 nm gold nanoparticle irradiated with a laser beam at a laser power density of 378 kW/cm² (~2 mW).

remove nonpolymerized molecule residuals and the resulting structure was analyzed by SEM (Figure 2a). The SEM micrographs revealed that a shell of PDMS was formed around the gold particles. For a constant laser power, the shell thickness increased with time and showed a saturation-like behavior for long exposure times (Figure 2c).

The same experiment was repeated for a constant exposure time but with an increasing laser power. Again, the sample was analyzed by SEM (Figure 2b). The PDMS shell around the particles showed a half-spherical, lens-shaped profile. The size of the polymer particles was increasing much more quickly and almost linearly with the laser power (Figure 2d). This could be explained, since the amount of light absorbed by the particles is also linearly dependent on the laser power and higher curing temperatures are therefore reached in a shorter amount of time. The half-spherical shape of the polymer shell also indicated that the heat around the nanoparticle is dissipating radially into the polymer cast. Finite element simulations were performed to estimate the heat distribution around the gold nanoparticle and the temperature levels at which the polymer was starting to cure under given experimental conditions. As shown in Figure 2e, the temperature distribution outside the gold nanoparticle is proportional to $I_0/(r \cdot k)$, where I_0 is the laser intensity, r is the distance to the center of the nanoparticle, and k is the thermal conductivity of the surrounding material.²⁶ We also performed numerical simulations to determine how fast the temperature is distributed at the particle surface (Supporting Information, Figure S2), showing that the high thermal conductivity and heat capacity of gold lead to an almost instantaneous and homogeneous temperature distribution around the gold particle within nanoseconds, even if the laser does not exactly heat the particle at the center. An 82 nm gold nanoparticle is therefore almost instantly heated up to 340 °C upon irradiation with a 2 mW laser. At a distance of 80 nm from the particle edge the temperature dropped to 78.9 °C and down to 47.7 °C at a distance of 170 nm, which corresponds to the shell thickness of PDMS for an exposure time of 16 s.

Importantly, the curing of PDMS was only achieved in presence of a gold particle and was not due to photo cross-linking by just irradiating the polymer precursor film with the laser alone. For this case, no structure formation was observed even at laser intensities that were more than 150 times higher in comparison to the heating experiments shown in Figure 2. This is in accordance with previous reports on the direct micro-patterning of PDMS with laser light, where PDMS cross-linking was only achieved by 2 photon absorption at laser powers and photon flux densities that were higher than those reported here.²⁷ The control experiment with the cw laser at high laser intensities but in the absence of a gold particle also indicates that the

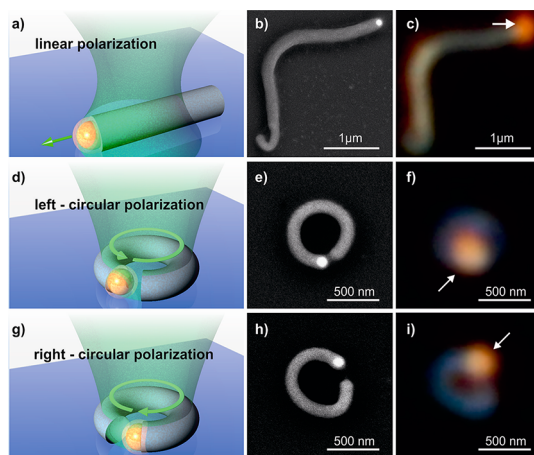


Figure 3. Fabrication of PDMS nanowires. (a) Schematic illustration of the nanowire formation with a linear polarized laser beam. The focused beam is pushing the gold nanoparticle over the surface of the substrate along a straight line. The sample is moved using an xyz microscope stage. (b) SEM and (c) DFM pictures of the nanowire structure. In both cases, the nanoparticle is clearly visible at the end of the PDMS wire (white arrow). Schematic illustration of the nanowire formation with (d) left circularly and (g) right circularly polarized light. (e) SEM and (f) dark-field images of a PDMS-wire made with left circularly polarized light. (h) SEM and (i) dark field images of the nanowire generated with right circularly polarized light. Again, the nanoparticles that were used to form the wires are visible at the end of the structures (white arrows).

PDMS curing is caused by heating and not by a photoinduced chemical reaction due to the enhanced local electromagnetic field around the particle.^{28,29} Numerical simulations showed an only 4-fold enhancement of the electromagnetic field for an 80 nm gold nanoparticle embedded in a polymer matrix (Supporting Information, Figure S3). Considering the high laser intensities used for the control experiment, the local near-field intensity would thus be insufficient to initiate a photoreaction of the PDMS precursor molecules at the same laser intensities that were used for plasmonic heating.

In the next step, the particle was heated and moved at the same time by the laser beam with the intention to form a nanowire (Figure 3a). This configuration is the analogue to the movement of the tip in a conventional scanning probe experiment, except that only optical forces are used to move the nanoparticle and no mechanical connection between the probe (here the gold nanoparticle) and the microscope is required.

For this experiment, a linearly polarized laser (power 1 mW, laser power density $<190 \text{ kW/cm}^2$) was focused slightly above the surface of the glass cover slip and moved laterally toward the particle by moving the microscope stage. The particle was pushed along the surface of the glass cover slip as soon as the laser was interacting with the particle. At the same time, the polymer blend started to polymerize within milliseconds along the track of the hot particle. The samples were rinsed with hexane and analyzed by SEM and

dark field microscopy (Figure 3b,c). PDMS nanowires with a diameter of \sim 120–130 nm and a length of several micrometers were formed on the surface. The direction of the nanowire was controlled by the movement of the microscope stage. Here, the use of a dark field microscope setup to study the nanostructure formation also proved to be a major advantage, since both the particles and the nanowire are visible by scattered light. The direction of the particle movement, the polymerization reaction, and the size and shape of the PDMS nanostructure can thus be directly observed during and after the experiment.

Forming a nanowire required a fine adjustment of the laser power to avoid that the particle would heat up too strongly and too quickly, which in turn leads to an almost instantaneous curing of the polymer resin. In that case, a thick polymer shell would form around the particles and fix them on the substrate. We therefore optimized the experimental conditions such that the laser power was sufficiently high to move the particles and to start the polymerization reaction but at the same time low enough to avoid the particle getting stuck. In the next step, we repeated the experiment with circularly polarized light to investigate whether the direction of the particle movement is also dependent on the polarization of the laser. A circularly polarized, strongly focused Gaussian beam, for example, carries a spin angular momentum^{30,31} which is converted to the orbital angular momentum³² and can be transferred to micrometer-sized metal particles³³ and polystyrene spheres.³⁴

In this case, the SEM and dark field analysis of the sample showed that the use of circularly polarized laser light caused the formation of ring-shaped structures (Figure 3d–i). The circular orientation of the ring was thereby polarization dependent, which led to the formation of right- and left-handed, chiral nanostructures with a single nanoparticle at the end of each wire, as shown in Figure 3d–i. Particles irradiated with right circularly polarized light were thereby moving clockwise (Figure 3d–f), while particles irradiated with left circularly polarized light were moving counterclockwise (Figure 3g–i) on the substrate. The ring structures were formed within milliseconds, and the diameter of the ring was dependent on the position of the nanoparticle with respect to the laser focus. The ring structure also showed a slightly different scattering than the PDMS wires made with linearly polarized light. This difference is likely caused by the wire growth being controlled merely by light and the wires being generated more quickly in comparison to the wires made with linearly polarized light, where the growth direction was controlled by moving the microscope stage.

The effect of circularly polarized light and the formation of a ring structure suggest a mechanism for the nanowire formation where the particle is simultaneously

pushed and heated by the laser beam at a temperature that is sufficiently high to cure the PDMS blend along the particle track. At the same time, the temperature of the particle has to be low enough to ensure that the hardening of PDMS is slightly delayed in comparison to the particle movement and that the particle is not embedded in a polymer shell. Considering that the temperature at the particle surface is also homogeneously equilibrating within nanoseconds (Figure S2, Supporting Information), this mechanism is more likely compared to a scenario where the polymerization reaction would start on one side of the particle and the hardening of the polymer cast would then push the particle forward. In this case, no polarization dependence for the wire formation should be expected.

We also performed a control experiment to prove that the particle movement in the polymer resin is caused by optical forces alone and that polymer curing is not the driving force of the particle motion. For this experiment, a single gold particle was immersed in a film of polymer precursor molecules but without adding a curing agent to the resin. No polymerization reaction that could interfere with the particle movement was observed under these conditions, due to the lack of cross-linker molecules. The particles, however, could be moved by the laser along the substrate over a distance of several micrometers (Supporting Information, Figure S4).

We performed numerical simulations of the optical forces exerted by a linearly polarized laser beam in order to get a better understanding of the driving force and the mechanism of the nanoparticle movement (Figure 4). As mentioned earlier, optical forces divide into scattering and gradient forces. The scattering forces are pointing along the axis of the energy flux of the light beam while the gradient force is pointing toward or away from the beam center in an axial direction, depending on whether the value of the force is positive or negative.²⁰ Positive gradient forces can be used to trap dielectric particles in the focus of a laser beam, but negative gradient forces just affect the opposite. Close to the plasmon frequency, scattering and absorption of light by the particle becomes increasingly important and these forces, expressed by the imaginary part of the particle polarization, are therefore dominating (Figure 4a,b). The particle is thus pushed along the direction of the beam propagation by a forward-directed force (Figure 4c). Notably, the gradient force, expressed by the real part of the particle polarization, has a negative value at the laser wavelength used in our experiments, which was slightly blue-shifted from the particle resonance wavelength (\sim 570 nm). The particle interacting with the laser beam is therefore subject to a negative gradient force which is pushing it out of the laser focus and along the surface of the substrate (Figure 4d).

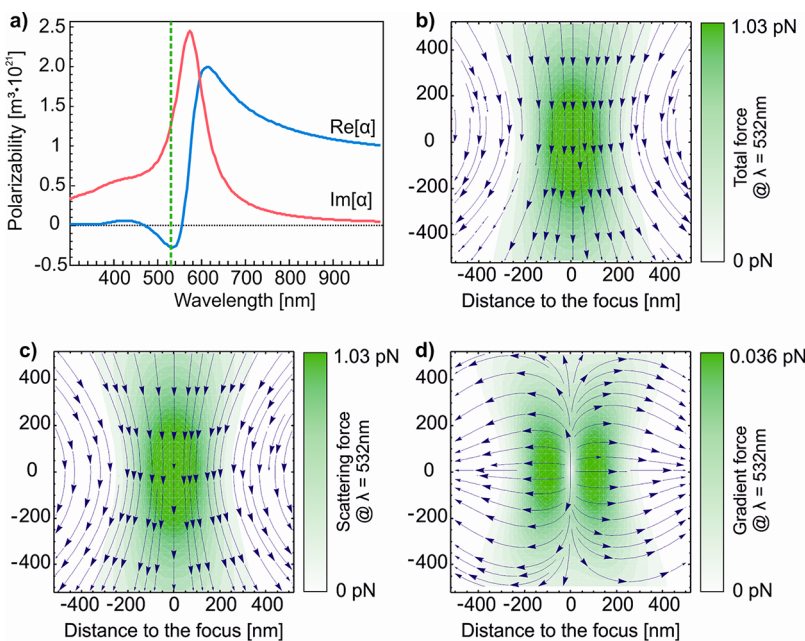


Figure 4. Complex polarizability of an 82 nm gold nanoparticle in PDMS ($n = 1.43$). (a) The real part of the particle polarization is negative at a wavelength that is slightly blue-shifted from the plasmon resonance frequency. The laser wavelength used in the experiments is indicated by the green dotted line. The gradient force at the wavelength used for nanowire formation is therefore negative and points away from the center of the laser focus. (b) Map of the total force (sum of scattering and gradient force) acting on a gold nanoparticle for $\lambda = 532$ nm and $P = 1$ mW. (c) Map of the scattering force and (d) map of the gradient force acting on the gold nanoparticle upon laser irradiation.

CONCLUSIONS

In summary, we have shown that plasmonic heating of gold nanoparticles can be used to control thermal curing of PDMS at the nanoscale. The applicability of this approach for nanofabrication was demonstrated by the synthesis of nanoparticles and nanowires. For a laser wavelength that is far red-shifted from the plasmon resonance, the gradient force acting on the gold particle would become positive while the scattering forces would be small. In this case the particle is pulled into the laser focus, which effectively leads to optical

trapping. Trapping the particle could be exploited to realize three-dimensional nanofabrication. Furthermore, splitting the laser beam into multiple beams by using a spatial light modulator would be a straightforward approach to increase the sample rate of the experiment, similar to the idea of using a multtip AFM cantilever for dip-pen lithography.³⁵ These further improvements could lead to the generation of larger structures such as nanofiber networks with subdiffractation limited resolution and pave the way to a new form of optical nanolithography in 3D.

MATERIALS AND METHODS

Materials. Au-NP in water (82 nm) was purchased from Nanopartz Inc. Glass substrates were purchased from Karl Hecht GmbH and cleaned with isopropyl alcohol and water before use. The PDMS elastomer-kit Sylgard 184 was purchased from Dow Corning, USA.

Instrumentation. An upright dark field microscope (Axiovert 100, Carl Zeiss Microscopy, LLC) with a $100\times$ air objective (Carl Zeiss Microscopy, LLC) and a numerical aperture of 0.9 was used as the basis for the measurements. A 532 nm cw laser (Millenia V, Spectra Physics) was coupled into the microscope. SEM measurements were performed in a scanning electron microscope (Zeiss Ultra55). Samples were made conductive by a thin layer of carbon to avoid charging of the sample during electron microscopy.

Simulations. Calculations of the gold particle temperatures and heat distribution were performed by finite elements simulation (Comsol Multiphysics). The calculation requires the absorption cross section of the nanoparticle, laser power density, and thermal capacity and heat conductance of the materials. The absorption cross section of gold nanoparticles in PDMS is calculated using Mie theory (MQMie, Dr. Michael Quinten).

The laser power density was calculated by first measuring the focused laser spot image and fitting a two-dimensional Gaussian function. We assume that the measured laser intensity is distributed over this function and the nanoparticle is placed exactly in the middle of the Gaussian beam. Integrating over the absorption cross section of the gold nanoparticle gives us the value for the laser power density (378 kW/cm² for 2 mW and 945 kW/cm² for 5 mW laser power). The values for material constants are taken from the literature: PDMS thermal conductivity, 0.17–0.18 W/(m K);³⁶ PDMS heat capacity, 1.799 kJ/(kg K);³⁷ PDMS refractive index, 1.4348;³⁸ Au dielectric constant.³⁹

Conflict of Interest: The authors declare no competing financial interest.

Acknowledgment. Financial support by the German Research Foundation (DFG) through the Nanosystems Initiative Munich (NIM), by the ERC through the Advanced Investigator Grant HYMEM, and by the DFG through the SFB 1032, project A8, is gratefully acknowledged.

Supporting Information Available: Figures giving measured and calculated extinction spectra of an 82 nm gold nanoparticle,

simulation of the temperature distribution around a gold nanoparticle, calculated electric field distribution, and dark-field image sequence of a gold nanoparticle moved by a laser beam. This material is available free of charge via the Internet at <http://pubs.acs.org>.

REFERENCES AND NOTES

- Gates, B. D.; Xu, Q.; Stewart, M.; Ryan, D.; Willson, C. G.; Whitesides, G. M. New Approaches to Nanofabrication: Molding, Printing, and Other Techniques. *Chem. Rev.* **2005**, *105*, 1171–1196.
- Piner, R. D.; Zhu, J.; Xu, F.; Hong, S.; Mirkin, C. A. Dip-Pen Nanolithography. *Science* **1999**, *283*, 661–663.
- Liu, G.-Y.; Xu, S.; Qian, Y. Nanofabrication of Self-Assembled Monolayers Using Scanning Probe Lithography. *Acc. Chem. Res.* **2000**, *33*, 457–466.
- Crommie, M. F.; Lutz, C. P.; Eigler, D. M. Confinement of Electrons to Quantum Corrals on a Metal Surface. *Science* **1993**, *262*, 218–220.
- Mamin, H. J.; Rugar, D. Thermomechanical Writing with an Atomic Force Microscope Tip. *Appl. Phys. Lett.* **1992**, *61*, 1003–1005.
- Minne, S. C.; Manalis, S. R.; Atalar, A.; Quate, C. F. Independent Parallel Lithography Using the Atomic Force Microscope. *J. Vac. Sci. Technol., B: Microelectron. Nanometer Struct.–Process., Meas., Phenom.* **1996**, *14*, 2456–2461.
- Wang, D.; Kodali, V. K.; Underwood, W. D., II; Jarvholm, J. E.; Okada, T.; Jones, S. C.; Rumi, M.; Dai, Z.; King, W. P.; Marder, S. R.; et al. Thermochemical Nanolithography of Multi-functional Nanotemplates for Assembling Nano-Objects. *Adv. Funct. Mater.* **2009**, *19*, 3696–3702.
- Riehn, R.; Charas, A.; Morgado, J.; Cacialli, F. Near-Field Optical Lithography of a Conjugated Polymer. *Appl. Phys. Lett.* **2003**, *82*, 526–528.
- Dryakhlushin, V. F.; Klimov, A. Y.; Rogov, V. V.; Vostokov, N. V. Near-Field Optical Lithography Method for Fabrication of the Nanodimensional Objects. *Appl. Surf. Sci.* **2005**, *248*, 200–203.
- Salaita, K.; Wang, Y.; Fragala, J.; Vega, R. A.; Liu, C.; Mirkin, C. A. Massively Parallel Dip-Pen Nanolithography with 55 000-Pen Two-Dimensional Arrays. *Angew. Chem., Int. Ed.* **2006**, *45*, 7220–7223.
- McCord, M. A. Electron Beam Lithography for 0.13 μ m Manufacturing. *J. Vac. Sci. Technol., B* **1997**, *15*, 2125–2130.
- Melngailis, J. Focused Ion Beam Technology and Applications. *J. Vac. Sci. Technol., B* **1987**, *4*, 469–495.
- Ashkin, A.; Dziedzic, J. M.; Bjorkholm, J. E.; Chu, S. Observation of a Single-Beam Gradient Force Optical Trap for Dielectric Particles. *Opt. Lett.* **1986**, *11*, 288–290.
- Baffou, G.; Quidant, R.; Girard, C. Heat Generation in Plasmonic Nanostructures: Influence of Morphology. *Appl. Phys. Lett.* **2009**, *94*, 153109–153109–3.
- Huang, X.; Jain, P. K.; El-Sayed, I. H.; El-Sayed, M. A. Plasmonic Photothermal Therapy (PPTT) Using Gold Nanoparticles. *Lasers Med. Sci.* **2008**, *23*, 217–228.
- Hrelescu, C.; Stehr, J.; Ringler, M.; Sperling, R. A.; Parak, W. J.; Klar, T. A.; Feldmann, J. DNA Melting in Gold Nanostove Clusters. *J. Phys. Chem. C* **2010**, *114*, 7401–7411.
- Cortie, M. B.; Harris, N.; Ford, M. J. Plasmonic Heating and Its Possible Exploitation in Nanolithography. *Phys. B (Amsterdam, Neth.)* **2007**, *394*, 188–192.
- Cao, L.; Barsic, D. N.; Guichard, A. R.; Brongersma, M. L. Plasmon-Assisted Local Temperature Control to Pattern Individual Semiconductor Nanowires and Carbon Nanotubes. *Nano Lett.* **2007**, *7*, 3523–3527.
- Walker, J. M.; Gou, L.; Bhattacharyya, S.; Lindahl, S. E.; Zaleski, J. M. Photothermal Plasmonic Triggering of Au Nanoparticle Surface Radical Polymerization. *Chem. Mater.* **2011**, *23*, 5275–5281.
- Dienerowitz, M.; Mazilu, M.; Dholakia, K. Optical Manipulation of Nanoparticles: a Review. *J. Nanophoton* **2008**, *2*, 021875–021875.
- Urban, A. S.; Lutich, A. A.; Stefani, F. D.; Feldmann, J. Laser Printing Single Gold Nanoparticles. *Nano Lett.* **2010**, *10*, 4794–4798.
- Fedoruk, M.; Lutich, A. A.; Feldmann, J. Subdiffraction-Limited Milling by an Optically Driven Single Gold Nanoparticle. *ACS Nano* **2011**, *5*, 7377–7382.
- Hansen, P. M.; Bhatia, V. K.; Harrit, N.; Oddershede, L. Expanding the Optical Trapping Range of Gold Nanoparticles. *Nano Lett.* **2005**, *5*, 1937–1942.
- Schmid, H.; Michel, B. Siloxane Polymers for High-Resolution, High-Accuracy Soft Lithography. *Macromolecules* **2000**, *33*, 3042–3049.
- Bhagat, A. A.; Jothimuthu, P.; Papautsky, I. Photodefinable Polydimethylsiloxane (PDMS) for Rapid Lab-On-A-Chip Prototyping. *Lab Chip* **2007**, *7*, 1192–1197.
- Govorov, A. O.; Zhang, W.; Skeini, T.; Richardson, H.; Lee, J.; Kotov, N. A. Gold Nanoparticle Ensembles as Heaters and Actuators: Melting and Collective Plasmon Resonances. *Nanoscale Res. Lett.* **2006**, *1*, 84–90.
- Coenjarts, C. A.; Ober, C. K. Two-Photon Three-Dimensional Microfabrication of Poly(Dimethylsiloxane) Elastomers. *Chem. Mater.* **2004**, *16*, 5556–5558.
- Hubert, C.; Romyantseva, A.; Lerondel, G.; Grand, J.; Kostcheev, S.; Billot, L.; Vial, A.; Bachelot, R.; Royer, P.; Chang, S.; Gray, S. K.; Wiederrecht, G. P.; Schatz, G. C. Near-Field Photochemical Imaging of Noble Metal Nanostructures. *Nano Lett.* **2005**, *5*, 615–619.
- Volpe, G.; Noack, M.; Acimovic, S.; Reinhardt, C.; Quidant, R. Near-Field Mapping of Plasmonic Antennas by Multiphoton Absorption in Poly(methyl methacrylate). *Nano Lett.* **2012**, *12*, 4864–4868.
- Simpson, S. H.; Hanna, S. Optical Angular Momentum Transfer by Laguerre-Gaussian Beams. *J. Opt. Soc. Am. A* **2009**, *26*, 625–638.
- Friese, M. E. J.; Nieminen, T. A.; Heckenberg, N. R.; Rubinsztein-Dunlop, H. Optical Alignment and Spinning of Laser-Trapped Microscopic Particles. *Nature* **1998**, *394*, 348–350.
- Nieminen, T. A.; Stilgoe, A. B.; Heckenberg, N. R.; Rubinsztein-Dunlop, H. Angular Momentum of a Strongly Focused Gaussian Beam. *J. Opt. A: Pure Appl. Opt.* **2008**, *10*, 115005–115005–6.
- Zhao, Y.; Shapiro, D.; McGloin, D.; Chiu, D. T.; Marchesini, S. Direct Observation of the Transfer of Orbital Angular Momentum to Metal Particles from a Focused Circularly Polarized Gaussian Beam. *Opt. Express* **2009**, *17*, 23316–23322.
- Ruffner, D. B.; Grier, D. G. Optical Forces and Torques in Non-uniform Beams of Light. *Phys. Rev. Lett.* **2012**, *108*, 173602–173602–4.
- Nedev, S.; Urban, A. S.; Lutich, A. A.; Feldmann, J. Optical Force Stamping Lithography. *Nano Lett.* **2011**, *11*, 5066–5070.
- Shin, Y. S.; Cho, K.; Lim, S. H.; Chung, S.; Park, S.-J.; Chung, C.; Han, D.-C.; Chang, J. K. PDMS-Based Micro PCR Chip with Parylene Coating. *J. Micromech. Microeng.* **2003**, *13*, 768–774.
- Yang, Y.-J.; Liao, H.-H. Development and Characterization of Thermopneumatic Peristaltic Micropumps. *J. Micromech. Microeng.* **2009**, *19*, 025003–025003–13.
- Schneider, F.; Draheim, J.; Kammerer, R.; Wallrabe, U. Process and Material Properties of Polydimethylsiloxane (PDMS) for Optical MEMS. *Sens. Actuators, A* **2009**, *151*, 95–99.
- Johnson, P. B.; Christy, R. W. Optical Constants of the Noble Metals. *Phys. Rev. B* **1972**, *6*, 4370–4379.